Contactless electroreflectance of AlGaN/GaN heterostructures deposited on *c*-, *a*-, *m*-, and (20.1)-plane GaN bulk substrates grown by ammonothermal method

R. Kudrawiec,[1,a)] M. Rudziński,[2] M. Gladysiewicz,[1] L. Janicki,[1] P. R. Hageman,[3]
W. Strupiński,[2] J. Misiewicz,[1] R. Kucharski,[4] M. Zając,[4] R. Doradziński,[4] and
R. Dwiliński[4]

[1]*Institute of Physics, Wroclaw University of Technology, Wybrzeże Wyspiańskiego 27, 50-370 Wrocław,
Poland*
[2]*Institute of Electronic Materials Technology, Wólczyńska 133, 01-919 Warsaw, Poland*
[3]*Institute for Molecules and Materials, Radboud University, Heyendaalseweg 135, 6525AJ Nijmegen,
The Netherlands*
[4]*AMMONO sp. z.o.o., Czerwonego Krzyża 2/31, 00-377 Warsaw, Poland*

Room temperature contactless electroreflectance (CER) has been applied to study optical transitions and the distribution of the built-in electric field in AlGaN/GaN heterostructures grown on *c*-, *a*-, *m*-, and (20.1)-plane GaN substrates obtained by the ammonothermal method. It has been clearly shown that polarization effects in the AlGaN/GaN heterostructures grown on the *c*-plane lead to a strong built-in electric field in the AlGaN layer. The aforementioned field was determined to be ∼0.43 MV/cm from the period of Franz–Keldysh oscillations (FKOs). In addition, polarization effects lead to the formation of a two dimensional electron gas at the AlGaN/GaN interface, which screens the band bending modulation in the GaN buffer layer, and, therefore, GaN-related excitonic transitions are not observed for this heterostructure. Such features/effects are also not observed in the AlGaN/GaN heterostructures grown on nonpolar and semipolar GaN substrates because any strong polarization effects are not expected in this case. For these heterostructures, very strong and sharp GaN excitonic resonances are clearly visible in CER spectra. The resonances are very similar to the excitonic transitions observed for the GaN epilayers deposited on nonpolar and semipolar substrates. Moreover, there is a very weak AlGaN-resonance without FKO for nonpolar and semipolar heterostructures instead of the strong AlGaN-related FKO, which is typical of polar AlGaN/GaN heterostructures. © *2011 American Institute of Physics*. [doi:10.1063/1.3560537]

I. INTRODUCTION

Due to strong spontaneous and piezoelectric polarization in III-N[1,2] a triangular quantum well is formed at the AlGaN/GaN interface when the heterostructure is grown along the polar direction ($+c$). Electrons accumulate at this interface forming a two dimensional electron gas (2DEG), which reaches a concentration of $\sim 10^{13}$ cm^{-2}, even without any intentional doping in the system.[2] Currently, this phenomenon is widely exploited in the field-effect transistor (FET) heterostructures operating with high powers at high temperatures.[3] However, this solution has some limitations because a large carrier density in the 2DEG is present even at the depletion mode. Some of these limitations can be overcome in the AlGaN/GaN heterostructures grown along nonpolar directions,[4–7] but this approach was not intensively explored because of the deficient access to native nonpolar GaN substrates. The recent progress in the ammonothermal growth of GaN crystals allows the fabrication of GaN substrates with various crystallographic orientations including polar and nonpolar as well as semipolar orientations.[8–11] It opens the possibility of the growth of AlGaN/GaN heterostructures along various crystallographic orientations in GaN. However, so far such studies were not intensively conducted, and a lot of fundamental properties are still unexplored for such heterostructures. One of them is the distribution of the built-in electric field in AlGaN/GaN heterostructures that is responsible for the formation of 2DEG at the AlGaN/GaN interface. In this paper, we applied contactless electroreflectance (CER) spectroscopy to study optical transitions and the built-in electric field in the AlGaN/GaN heterostructures grown by metalorganic chemical vapor deposition (MOCVD) on *c*-, *a*-, *m*-, and (20.1)-plane GaN substrates obtained by the ammonothermal method.

CER spectroscopy is a very powerful absorptionlike technique to study optical transitions in various semiconductor structures, including quantum dots,[12] quantum wells,[13] and FETs.[14–19] Its derivative character allows both the elimination of the background signal and detection of very weak optical transitions even at room temperature. Due to the Franz–Keldysh effect,[20] this method can be applied to investigate the built-in electric field in AlGaN/GaN transistor heterostructures[16–19] as well as the type of band bending.[19,21] CER spectroscopy has been applied many times to study optical transitions and the built-in electric field in polar AlGaN/GaN heterostructures.[16–19] It has been shown that
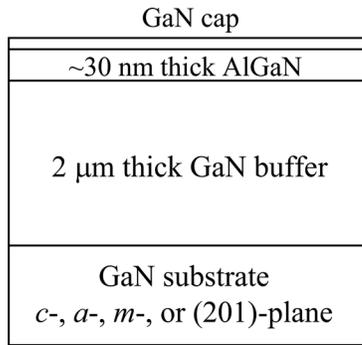

FIG. 1. Layer sequence in AlGaN/GaN heterostructures grown on bulk GaN substrates of various crystallographic orientations.

this technique enables detecting the formation of 2DEG at the AlGaN/GaN interface in a contactless manner[22] as well as determining the built-in electric field in the AlGaN barrier[16–19] and its changes upon SiN deposition.[17] Therefore, it is expected that CER spectroscopy will provide similar information for the AlGaN/GaN heterostructures grown on nonpolar and semipolar GaN substrates.

II. EXPERIMENTAL DETAILS

AlGaN/GaN heterostructures (see the layer sequence in Fig. 1) were grown by MOCVD (with a RF heated AIX-TRON AIX-200 low pressure horizontal reactor) simultaneously on c-, a-, m-, and (20.1)-plane GaN substrates obtained by the ammonothermal method. Trimethylgallium, trimethylaluminium, and ammonia were used as precursors and H_2 as the carrier gas. For comparison purposes, a set of 2 μm thick GaN layers were grown under the same conditions. CER measurements were performed at room temperature in a capacitor with the top electrode made from a copper-wire mesh, which was semitransparent for light. This electrode was kept at a distance of $\sim$0.5 mm from the sample surface, while the sample itself was fixed on the bottom copper electrode. A maximum peak-to-peak alternating voltage of $\sim$3.0 kV with the frequency of 285 Hz was applied. Other relevant details of CER measurements are described in Ref. 19.

III. RESULTS AND DISCUSSION

Figures 2(a)–2(d) show the CER spectra of the AlGaN/GaN heterostructure and GaN layer grown on the c-, a-, m-, and (20.1)-plane GaN substrate, respectively. To enable comparison between the above-mentioned CER spectra, the same scale and spectral range are used. The CER features related to GaN and AlGaN layers are observed for all heterostructures, but their shape and intensity strongly depend on the crystallographic orientation.

For the heterostructure grown on c-plane GaN [Fig. 2(a)], the spectrum is very similar to the CER spectra previously reported for AlGaN/GaN heterostructures, see Refs. 16–19, 21, and 22. The observed AlGaN signal possesses a characteristic Franz–Keldysh oscillation (FKO), the period of which depends on the built-in electric field in the AlGaN layer. A conventional method to determine the built-in electric field from FKO is to use an asymptotic expression for electro-reflectance[20]
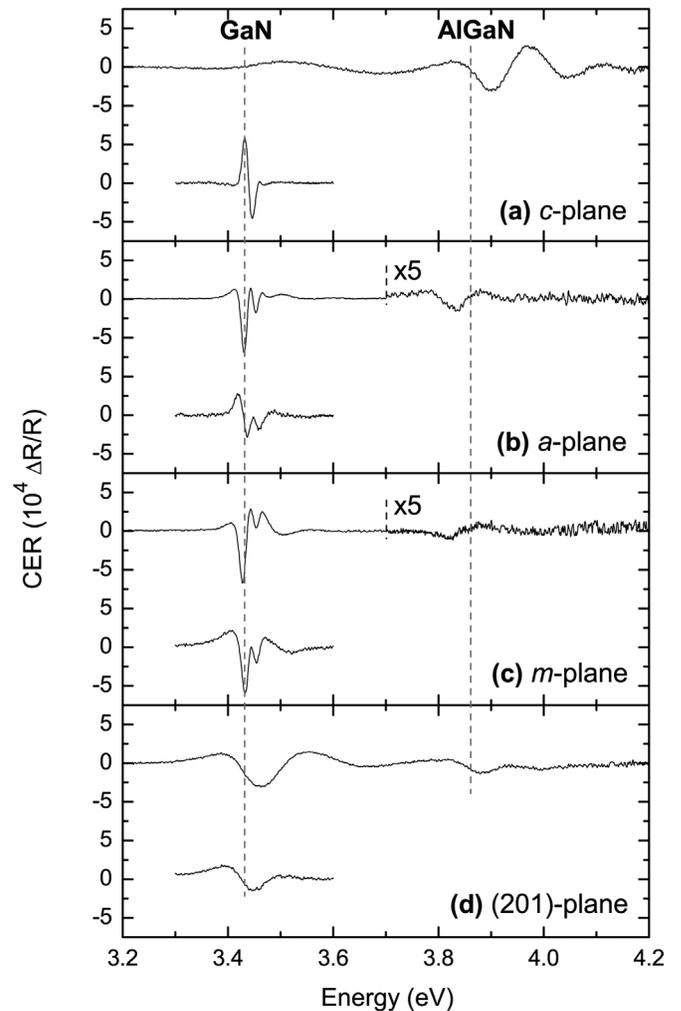

FIG. 2. Room temperature contactless electroreflectance spectra measured for AlGaN/GaN heterostructures (top spectra) and 2 μm thick GaN layers (bottom spectra) grown on (a) c-, (b) a-, (c) m-, and (d) (20.1)-plane bulk GaN substrates.

$$\frac{\Delta R}{R} \propto \exp\left[\frac{-2\Gamma\sqrt{E-E_g}}{(\hbar\theta)^{3/2}}\right] \cdot \cos\left[\frac{4}{3}\left(\frac{E-E_g}{\hbar\theta}\right)^{3/2}+\phi\right]$$
$$\times \frac{1}{E^2(E-E_g)}, \tag{1}$$
$$(\hbar\theta)^3 = \frac{e^2\hbar^2F^2}{2\mu},$$

where $\hbar\theta$ is the electro-optic energy, Γ is the line width, ϕ is an angle, F is the electric field, and μ is the electron-hole reduced mass (for AlGaN μ is assumed to be 0.2 m_0 after Ref. 23). The extrema of FKO are given by

$$n\pi = \phi + \frac{4}{3}\left[\frac{(E_n-E_g)}{\hbar\theta}\right]^{3/2}, \tag{2}$$

where n is the index of the nth extremum and E_n is the corresponding energy. A plot of $(E_n-E_g)^{3/2}$ versus n yields a straight line with a slope proportional to F. An analysis of the AlGaN-related FKO period for the AlGaN/GaN heterostructure grown on the c-plane GaN substrate is shown in Fig. 3. The built-in electric field in the AlGaN layer has been determined from this plot to be $\sim$0.43 MV/cm.
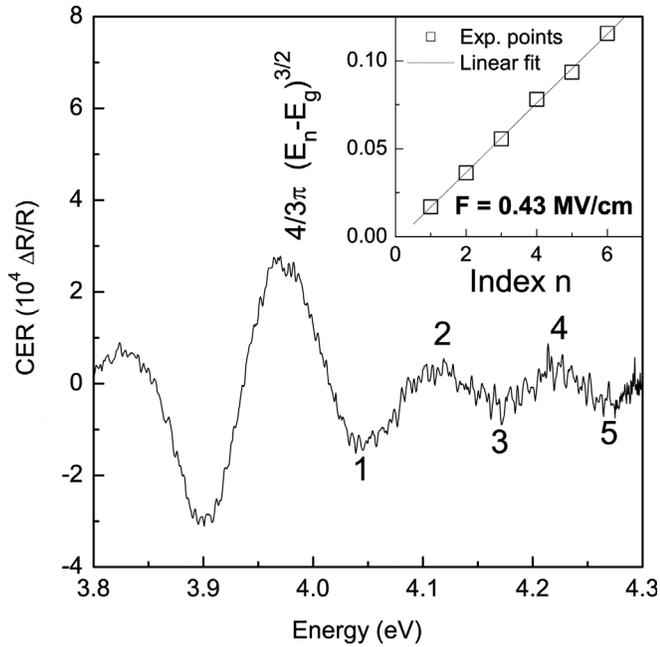
FIG. 3. Room temperature contactless electroreflectance spectrum of AlGaN/GaN heterostructure grown on *c*-plane GaN substrate in the vicinity of AlGaN transition together with the analysis of the period of Franz–Keldysh oscillation (inset).
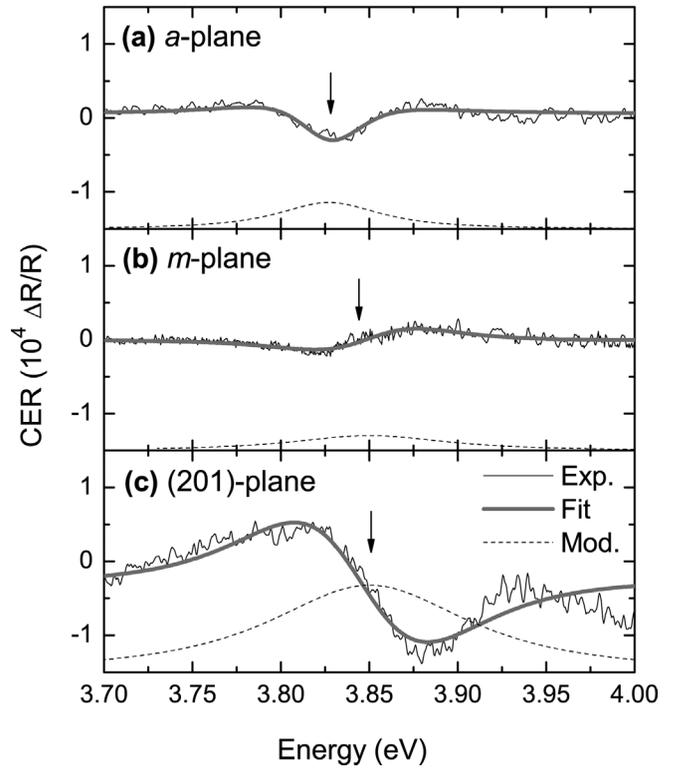

FIG. 4. Room temperature contactless electroreflectance spectra of AlGaN/GaN heterostructures grown on (a) *a*-, (b) *m*-, and (c) (20.1)-plane GaN substrate in the vicinity of AlGaN transition together with the fit (thick gray lines) by Eq. (3) and the moduli of CER resonances (dashed lines).

For the AlGaN/GaN heterostructures grown on nonpolar GaN substrates, any AlGaN-related FKOs are not observed in CER spectra. In this case, the shape of CER resonance is typical of an excitonic or band-to-band absorption in a layer with a weak built-in electric field. For such an absorption, the line shape of CER resonance is described by Aspnes formula[24]

$$\frac{\Delta R}{R}(E) = \mathrm{Re}\left[C \cdot e^{i \cdot \vartheta}(E - E_0 + i \cdot \Gamma)^{-m}\right], \quad (3)$$

where E_0 and Γ are the energy and the broadening parameter of the transition, and C and ϑ are the amplitude and phase of the resonance, respectively. The term m refers to the type of optical transitions and equals 2 for an excitonic and 2.5 for a band-to-band transition. Figures 4(a)–4(c) show the analysis of the AlGaN-related transition for heterostructures grown on *a*-, *m*,- and (20.1)-plane GaN substrates together with the fitting curves (thick gray lines) and the moduli of CER resonances (dashed lines), which are calculated from Eq. (4)

$$\Delta\rho(E) = \frac{|C|}{[(E - E_0)^2 + \Gamma^2]^{m/2}} \quad (4)$$

with parameters taken from the fit. It has been observed that the energy gap of the AlGaN layer grown simultaneously in the same process on GaN substrates with various crystallographic orientations is different. It means that the aluminum incorporation into the AlGaN alloy depends on the growth direction. This conclusion has been confirmed by x-ray diffraction measurements, and it will be discussed in detail elsewhere.

As seen in Fig. 2(a), GaN excitonic transitions are not observed for the polar AlGaN/GaN heterostructure, whereas

in the case of the GaN epilayer grown on the *c*-plane GaN as well as AlGaN/GaN heterostructures and GaN layers grown on nonpolar substrates they are clearly visible, see Fig. 2. This phenomenon is associated with the screening of band bending modulation in the GaN buffer layer by 2DEG.[16,22] Figure 5(a) schematically shows band bending and its modulation in the AlGaN/GaN heterostructure grown on the *c*-plane GaN. In addition, the possible optical transitions in each part of this structure are marked by arrows in this scheme, and their character is described in the figure caption. According to this sketch, excitonic transitions are expected far from the AlGaN/GaN interface where the band bending is weak, see the transition labeled as (iv) in Fig. 5(a). However, no band bending modulation is expected in this region because of the screening of electromodulation in this layer. It explains why excitonic transitions are not observed for this heterostructure. The weak and broad CER feature at $\sim 3.5 - 3.6$ eV [see Fig. 2(a)] is attributed to light absorption in the GaN cap layer (that is, it is an optical transition in the GaN surface quantum well[25]) and/or band-to-band absorption in the GaN buffer layer near the AlGaN/GaN interface, see (iii) arrows in Fig. 5(a).

The strong excitonic transitions in the AlGaN/GaN heterostructures grown on nonpolar substrates [see Figs. 2(b) and 2(c)] mean that the band bending in the GaN buffer layer is not strong because such sharp excitonic transitions are expected for layers with a weak band bending. In addition, it means that the band bending in the GaN buffer layer is effectively modulated in these samples (that is, no screening
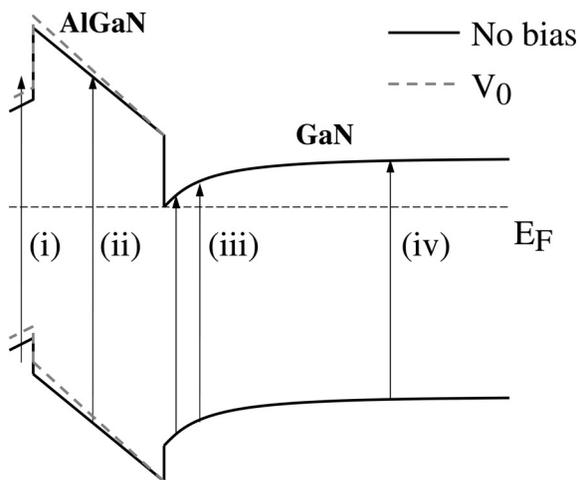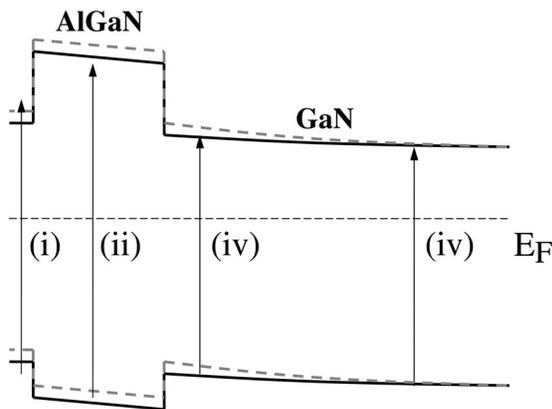
(a) Polar AlGaN/GaN heterostructure

(b) Unpolar AlGaN/GaN heterostructure

FIG. 5. Sketch of band bending and optical transitions in (a) polar and (b) nonpolar AlGaN/GaN heterostructures. (i) optical transition in GaN surface quantum well; (ii) band-to-band transition in AlGaN layer; (iii) band-to-band transition in GaN buffer layer; (iv) excitonic transition in GaN buffer layer.

phenomenon is present for these heterostructures because no 2DEG is expected at the AlGaN/GaN interface). In this case, the intensity of the CER signal is more or less proportional to the absorption volume, which is much larger for the GaN buffer layer than for the AlGaN layer, and, therefore, the intensity of the AlGaN transition is much weaker.

The lack of polarization effects along the nonpolar direction in III-N means that the surface band bending in nonpolar AlGaN/GaN heterostructures results from the Fermi-level pinning on the surface and the carrier concentration inside the structure. The band bending and its modulation for an unpolar heterostructure is plotted schematically in Fig. 5(b). In addition, the possible optical transitions are marked by arrows in this sketch. Very similar GaN excitonic transitions are expected for AlGaN/GaN heterostructures and GaN layers within the scheme. Such similarities are clearly visible by naked eye in Fig. 2. For a better comparison, CER spectra in the vicinity of GaN transitions have been fitted by Eq. (3), see Fig. 6. The excitons A and B are fitted by one resonance because the energy separation between these tran-
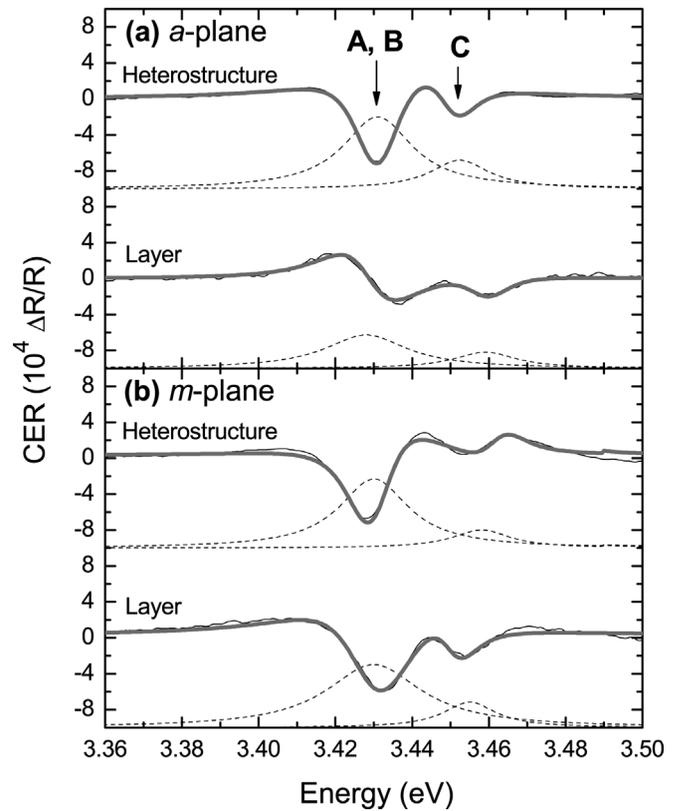

FIG. 6. Room temperature contactless electroreflectance spectra of AlGaN/GaN heterostructures and GaN epilayers grown on (a) *a*- and (b) *m*-plane GaN substrate in the vicinity of GaN transition together with the fit (thick gray lines) by Eq. (3) and the moduli of CER resonances (dashed lines).

sitions is much smaller than the broadening of individual exciton lines [5 meV (Ref. 26) vs ∼10–15 meV]. Within this analysis, very similar excitonic transitions have been identified as can be seen by comparing the moduli of excitonic resonances. The observed differences between the shape of CER resonances for the AlGaN/GaN heterostructure and the GaN layer (that is, various phases of these resonance) appear due to the distance of GaN buffer layer from the surface (that is, the presence of GaN cap and AlGaN layer).

For the AlGaN/GaN heterostructure grown on the semipolar GaN substrate, the GaN-related feature is quite broad. However, very similar resonance is also observed for the GaN epilayer with (20.1)-orientation, see Fig. 2(d). It suggests that the quality of the GaN layer grown along this crystallographic orientation is worse than the quality of GaN layers grown along polar and nonpolar directions. On the other hand, a built-in electric field is expected in this heterostructure, but the strong GaN related signal suggests that the 2DEG is rather not present at the AlGaN/GaN interface.

It is worth noting that for all AlGaN/GaN heterostructures, an optical transition in the GaN cap layer is also expected in CER spectra.[25] Because of quantum confinement, it is located at a higher energy position than that of the GaN energy gap. In our analysis, this transition is neglected because its intensity is much weaker than in the case of GaN excitonic transitions. Moreover, its broadening is quite large because of the width fluctuations of the cap layer. To illustrate this issue, a histogram of optical transitions for an
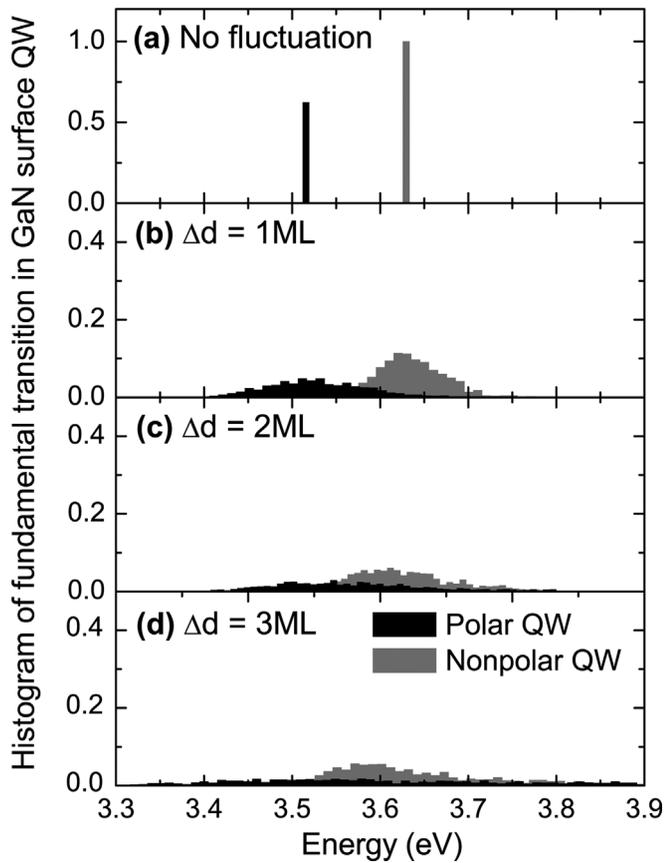
FIG. 7. Histogram of the ground state transition in 2 nm wide GaN surface QW with various inhomogeneities of QW width (Δd).

inhomogeneous GaN surface quantum well (QW) is calculated and presented in Fig. 7. These calculations were performed according to the model described in Ref. 27 in which the quantum width is treated as a random number with a Gaussian distribution, where the nominal cap width corresponds to the mean value in this distribution and the width fluctuation is the deviation from the main value. Figure 7 clearly shows that the broadening of QW transition increased, and its intensity decreased very significantly when the QW width fluctuation was increased. In our samples, the surface roughness can be even on the level of ∼2 monolayers (MLs). For such QW inhomogeneities, a very broad and weak CER resonance is expected, which is very consistent with our experimental data, see CER spectrum for the polar AlGaN/GaN heterostructure in Fig. 2(a).

IV. CONCLUSION

In conclusion, CER features typical of FET hetrostructures with a strong built-in electric field and 2DEG (that is, AlGaN-related FKO and the screening of band bending modulation in the GaN buffer layer) are observed only for the AlGaN/GaN heterostructures grown on the *c*-plane substrate. When the same AlGaN/GaN heterostructures are grown on nonpolar or semipolar GaN substrates, any CER features that could be related to a strong built-in electric field in the AlGaN layer or the 2DEG presence at the interface are not visible in CER spectra. It means that modula-

tion doping is necessary for nonpolar and semipolar AlGaN/GaN FET heterostructures and the total depletion of the 2DEG will be possible in such heterostructures.

[1]F. Bernardini and V. Fiorentini, Phys. Rev. B **64**, 085207 (2001).

[2]O. Ambacher, J. A. Majewski, C. Miskys, A. Link, M. Hermann, M. Eickhoff, M. Stutzmann, F. Bernardini, V. Fiorentini, V. Tilak, B. Schaff, and L. F. Eastman, J. Phys.: Condens. Matter. **14**, 3399 (2002).

[3]See, for example, the Proceeding of 8th International Conference on Nitride Semiconductors in Korea published in Phys. Status Solidi **7**, (2010).

[4]M. Kuroda, H. Ishida, T. Ueda, and T. Tanaka, J. Appl. Phys. **102**, 093703 (2007).

[5]S. L. Selvaraj and T. Egawa, Jpn. J. Appl. Phys. **47**, 3332 (2008).

[6]S. Arulkumaran, S. Lawrence Selvaraj, T. Egava, and G. I. Ng, Appl. Phys. Lett. **92**, 092116 (2008).

[7]C. Y. Chang, Y.-L. Wang, B. P. Gila, A. P. Gerger, S. J. Pearton, C. F. Lo, F. Ren, Q. Sun, Y. Zhang, and J. Han, Appl. Phys. Lett. **95**, 082110 (2009).

[8]R. Dwilinski, R. Doradzinski, J. Garczynski, L. Sierzputowski, R. Kucharski, M. Zajac, M. Rudzinski, R. Kudrawiec, J. Serafinczuk, and W. Strupinski, J. Cryst. Growth **312**, 2499 (2010).

[9]R. Kucharski, M. Rudzinski, M. Zaj[ogon]ac, R. Doradzinski, J. Garczynski, L. Sierzputowski, R. Kudrawiec, J. Serafinczuk, W. Strupinski, and R. Dwilinski, Appl. Phys. Lett. **95**, 131119 (2009).

[10]R. Kudrawiec, M. Rudzinski, R. Kucharski, M. Zajac, R. Doradzinski, L.P. Sierzputowski, J. Rarczynski, J. Serafinczuk, W. Strupinski, J. Misiewicz, and R. Dwilinski, Phys. Status Solidi C **7**, 2359 (2010).

[11]R. Kucharski, M. Zajac, R. Doradzinski, J. Graczynski, L. Sierzputowski, R. Kudrawiec, J. Serafinczuk, J. Misiewicz, and R. Dwilinski, Appl. Phys. Express **3**, 101001 (2010).

[12]M. Munoz, S. Guo, X. Zhou, M. C. Tamargo, Y. S. Huang, C. Trallero-Giner, and A. H. Rodriguez, Appl. Phys. Lett. **83**, 4399 (2003); M. Motyka, R. Kudrawiec, G. Sek, J. Misiewicz, I. L. Krestnikov, S. Mikhrin, and A. Kovsh, Semicond. Sci. Technol. **21**, 1402 (2006); M. Motyka, R. Kudrawiec, G. Sek, J. Misiewicz, D. Bisping, B. Marquardt, A. Forchel, and M. Fischer, Appl. Phys. Lett. **90**, 221112 (2007).

[13]R. Kudrawiec, M. Gladysiewicz, J. Misiewicz, F. Ishikawa, and K. H. Ploog, Appl. Phys. Lett. **90**, 041916 (2007); R. Kudrawiec, M. Gladysiewicz, J. Misiewicz, H. B. Yuen, S. R. Bank, M. A. Wistey, H. P. Bae, and J. S. Harris, Jr., Phys. Rev. B **73**, 245413 (2006).

[14]Y. S. Huang, W. D. Sun, F. H. Pollak, J. L. Freeouf, I. D. Calder, and R. E. Mallard, Appl. Phys. Lett. **73**, 214 (1998).

[15]D. Y. Lin, Y. S. Huang, T. S. Shou, K. K. Tiong, and F. H. Pollak, J. Appl. Phys. **90**, 6421 (2001).

[16]R. Kudrawiec, M. Syperek, M. Motyka, J. Misiewicz, R. Paszkiewicz, B. Paszkiewicz, and M. Tłaczała, J. Appl. Phys. **100**, 013501 (2006).

[17]R. Kudrawiec, B. Paszkiewicz, M. Motyka, J. Misiewicz, J. Derluyn, A. Lorenz, K. Cheng, J. Das, and M. Germain, J. Appl. Phys. **104**, 096108 (2008).

[18]D. Y. Lin, J. D. Wu, J. Y. Zheng, and C. F. Lin, Physica E **40**, 1763 (2008).

[19]R. Kudrawiec, Phys. Status Solidi B **247**, 1616 (2010).

[20]D. E. Aspnes and A. A. Studna, Phys. Rev. B **7**, 4605 (1973); H. Shen and M. Dutta, J. Appl. Phys. **78**, 2151 (1995).

[21]R. Kudrawiec, M. Motyka, J. Misiewicz, B. Paszkiewicz, R. Paszkiewicz, and M. Tłaczała, Microelectron. J **40**, 370 (2008).

[22]M. Motyka, R. Kudrawiec, M. Syperek, J. Misiewicz, M. Rudzinski, P. Hageman, and P. K. Larsen, Thin Solid Films **515**, 4662 (2007).

[23]I. Vurgaftman and J. R. Meyer, J. Appl. Phys. **94**, 3675 (2003).

[24]D. E. Aspnes, Surf. Sci. **37**, 418 (1973).

[25]M. Motyka, M. Syperek, R. Kudrawiec, J. Misiewicz, M. Rudzinski, P. R. Hageman, and P. K. Larsen, Appl. Phys. Lett. **89**, 231912 (2006);

R. Kudrawiec, M. Gladysiewicz, J. Misiewicz, R. Paszkiewicz, B. Paszkiewicz, and M. Tlaczala, AIP Conf. Proc **1199**, 25 (2009).

[26]R. Kudrawiec, M. Rudzinski, J. Serafinczuk, and M. Zajac, J. Appl. Phys. **105**, 093541 (2009).

[27]M. Gladysiewicz and R. Kudrawiec, J. Phys.: Cond. Mater. **22**, 485801 (2010).